Wear 456–457 (2020) 203401

Contents lists available at ScienceDirect

Wear

journal homepage: http://www.elsevier.com/locate/wear

A heuristic wear model for the contact strip and contact wire in pantograph – Catenary interaction for railway operations under 15 kV 16.67 Hz AC systems

Stefano Derosa [a,*], Petter Nåvik [a], Andrea Collina [b], Giuseppe Bucca [b], Anders Rønnquist [a]

[a] Department of Structural Engineering, Norwegian University of Science and Technology, Trondheim, Norway
[b] Department of Mechanical Engineering, Politecnico di Milano, Milan, Italy

ARTICLE INFO

Keywords:
Railway catenary systems
Pantograph-catenary sliding contact
Copper wire wear model
Carbon strip wear model

ABSTRACT

The sliding contact between the pantograph and catenary allows the correct operation of electric trains. However, this contact induces wear on both the components involved in the process, namely the contact strip on the pantograph and the contact wire on the catenary. The influence of operating parameter values (i.e., the fed current intensity, uplift force and train speed) has recently gained attention, with the aim of creating wear models for both parts involved in the contact. In this study, a procedure assessed in the literature is adapted to operating conditions with AC catenary systems at 15kV/16.67 Hz and Cu-impregnated carbon contact strips. The resulting models are suitable for the wear prediction of both the contact wire and the contact strip.

1. Introduction

Electric trains rely on a complex system to collect the electricity needed to run. A commonly used system is composed of two main parts, one fixed to the ground and one moving with the train, with the intention of keeping constant contact at all times. The first subsystem is the power feeding subsystem, namely, the catenary infrastructure, and the second subsystem is the power collection subsystem, namely, the pantograph. To guarantee smooth and reliable operations, this contact must always be ensured. A large number of publications on the topic of pantograph-catenary interaction [1] show how the research focus is mainly on finding solutions to reduce the variability of the contact force between the pantograph and catenary, hence improving the contact quality. However, the constant contact between two sliding components comes at the cost of their wear. The first wear influencing factors that were studied were the materials chosen for the wire and contact strip [2]. Later, operational parameters such as the train speed, current intensity and contact force were investigated, broadening the knowledge on the phenomenon. It is beneficial to emphasize that while the train speed and current intensity are parameters that can be set individually, the contact force between the wire and the pantograph is the result of the dynamics associated with the pantograph-catenary interaction [3]. Hence, the contact force is influenced by multiple factors related to the catenary system. Given the difficulty of obtaining significant results from field data, analysis through specifically designed test rigs has become the best practice [4]. In this way, it is possible to conduct controlled measurements that are accurate and to explore variations within the range of the operational parameters. It is important to point out, however, that this type of test is inherently more difficult to transfer to field operations than other types of test [5] due to the way the test setup is designed [6]. Various investigations have focused on finding the effects on the wear of the current intensity and train speed [7], contact force and dwell time [8], and "current lubrication" effect [9]. Specific studies have been conducted in both AC [10] and DC [11] configurations on the arcing phenomenon, which may induce serious damage if not properly controlled. The influence of the material has been analysed through testing contact strips made of pure carbon [12], copper-impregnated carbon [13], iron-base [14] and carbon composite [15] and through verifying the cases in which lubricants have a positive influence [16]. The amount of research focused on the effects of single parameters shows how difficult it is to have a validated model that relates the wear to the material properties and the operating conditions [4]. A solution based on the concept of wear maps [17] was proposed in Ref. [18], and a heuristic model for the contact wire wear was presented in Ref. [19] for the DC case, as a further development of the first model introduced in Ref. [20]. Concerning the contact strip, the study

* Corresponding author.
E-mail address: stefano.derosa@ntnu.no (S. Derosa).

https://doi.org/10.1016/j.wear.2020.203401
Received 2 April 2020; Received in revised form 16 June 2020; Accepted 2 July 2020
Available online 6 July 2020

described in Ref. [21] gives the possibility to evaluate the wear within the same range of values of current and force as in the contact wire wear model in Ref. [19].

The aim of this study is to provide a heuristic model for the wear of both the contact wire and the contact strip and to further increase the understanding of the wear phenomenon on the two components. The working conditions for the models are referred to as a 15 kV 16.67 Hz AC catenary system and a Cu-impregnated contact strip, thus corresponding to the working conditions for the railways in Norway [22]. To achieve the desired result, an analysis procedure has been built following the state of the art in the field. The first step involves a dedicated set of laboratory tests, described in chapter 2, where a 100 mm^2 cross-section CuAg contact wire and copper-impregnated carbon contact strips are used. This allows recreating the same pantograph-catenary couple as the one currently in use on the main electric lines in Norway. Each of the tests was designed for the investigation of specific operating conditions, namely the train speed, the current intensity and the contact force. The range chosen for these three parameters exceeds the values currently in use, extending the analysis to new possible combinations that apply to future operating conditions. In this way, it is possible to predict the expected behaviour for new or improved existing lines. Each combination of parameters was tested once, giving priority to the investigation of different testing conditions of the wear model over the repetition of the same test multiple times. The test results were then used to generate the model. Starting from the findings of a project focused on wire wear for the DC case [19], an extension to the AC case has been performed. Furthermore, a model for the contact strip has been formulated, adjusting the procedure to the effects that influence the contact strip wear. It is important to underline, at this point, that the resulting model will be specific for this system, namely this type of contact wire and this type of contact strip. In case a model is needed for a different couple of materials, the same procedure presented in this paper needs to be followed with a dedicated set of experiments and the relative equation adaptation. Chapter 3 explains how the model works, and chapters 4 and 5 respectively explain the procedures adopted to tune the model for the contact wire and the contact strip. A comparison of the models is presented in chapter 6, and conclusions are drawn in chapter 7.

2. Laboratory tests

The experimental tests were carried out in Italy at Politecnico di Milano. At the Department of Mechanical Engineering laboratories, there is an existing test rig that was used to execute all the planned test variations, spanning nominal contact forces between 60 N and 90 N, 16.67 Hz AC with an intensity between 300 A and 400 A, and train speeds of up to 210 km/h. The configuration of this test rig allows for test conditions that are very close to the ones found in the field. To reproduce the train speed, a 2.2 m radius fibreglass wheel rotates with the contact wire mounted on the edge of the wheel via 36 elastic supports. The change in the horizontal position associated with the contact wire stagger is also reproduced, via a linear actuator that moves the contact strip back and forth in the radial direction with respect to the wheel, i.e., perpendicular to the wire. An air duct positioned in front of the contact strip provides adequate airflow to replicate the flow the pantograph would experience if running with the same conditions on a railway line. A complete and thorough explanation of the test rig characteristics can be found in Ref. [4].

During each test, a set of force transducers placed on the mounting platform for the contact strip allowed to record vertical and longitudinal contact forces, and an accelerometer placed at the centre of the contact strip provided the vertical acceleration time history. Further measurements related to the current and voltage were taken, allowing the evaluation of the electrical resistance at the contact point, which is known to vary with the level of the contact force [23]. The voltage signal is also used to calculate the percentage of contact loss during the test.

Each test run corresponded to 3000 km, a distance that provides enough wear to the contact wire to make measurements possible. Given the complexity of the test rig and the values of force, speed and electrical power involved, the test duration was ca. four days for the longest tests and ca. two days for the shortest.

The wear assessment is carried out in a specific way for the contact wire (Fig. 1(a)) and contact strip (Fig. 1(b)). For the latter, the evaluation is performed on the sample mass, measured by means of a digital scale with an accuracy of 0.1 g before and after the test. Thus, the loss of mass per kilometre for the contact strip is averaged over the running distance. Regarding the contact wire, a more complex procedure is required since the amount of wear is given by the reduction in the thickness of the wire itself. The thickness is also measured before and after each test, but in contrast to the contact strip, this evaluation is done in multiple locations along the wire to account for the different levels of wear associated, for example, with different levels of stiffness. The thickness is measured through a laser system with an accuracy of approximately 3 μm at 180 different points evenly spaced along the contact wire. With the geometric characteristics of the wire, namely, the cross-section and the thickness, the amount of area removed per million pantograph passages is then obtained.

The list of tests included a base case test, used as a reference for comparison with all other tests. The base case is needed because of the inherent differences that lie between the laboratory experiments and the field measurements. It is not possible to transfer the result directly from the laboratory to the field case. However, it is possible to relate to the variations between the different cases. For this set of experiments, the base case was characterized by a current intensity of 300 A (AC 16.67 Hz), an uplift force of 60 N and a train speed of 210 km/h. It is important to emphasize that for the current intensity and uplift force, the value refers to each contact strip. In the case of a pantograph with multiple contact strips, the value must be modified accordingly. From the base case, all other cases were designed by changing one parameter at a time to obtain a distribution of values within the range of interest. To investigate the current situation in Norway regarding the train speed, values of 130 km/h and 160 km/h were chosen. These are the speeds commonly used on the electric lines, with the 210 km/h value chosen for the base case corresponding to the newly designed lines maximum speed. The current intensity value of the base case (300 A), on the other hand, represents the standard value for the railways, and higher values of 350 A and 400 A were chosen for the study. The contact force values chosen for the further tests were higher than the base case, 75 N and 90 N, to assess how much the wear is influenced by an increased force acting between the pantograph and the catenary.

3. The wear model

This chapter explains the model chosen to describe the wear in the contact wire and contact strip. When a reliable model is defined, it is possible to obtain wear values within the validity range without the need for further tests. Since the test duration is lengthy and measurements are subjected to errors, having such a model is of great benefit. To fit the results to a model, a hypothesis is needed regarding the contributing effects to the wear. Literature reports [19] show that there are two main contributors to the phenomenon: mechanical and electrical. Mechanical wear is a consequence of the contact wire and the contact strip sliding against each other. To ensure that this contact is maintained the whole time, for electrical continuity purposes, the contact strip is pushed against the contact wire, hence forming a sliding contact. Electrical wear, on the other hand, is due mainly to the Joule effect. In addition, arcs originating between the contact wire and the contact strip whenever contact is lost contribute to material erosion. The loss of contact is an undesired effect that occurs because of the dynamic of the interaction between pantograph and catenary. All the efforts from both the train operators and the infrastructure owners are oriented towards the loss of contact not occurring, but this effect is always present, so it must be considered.

Fig. 1. CuAg 100 mm^2 section contact wire (a) and copper-impregnated carbon contact strip (b) used during the laboratory tests.

A formula based on a long series of experiments was proposed in Ref. [19]. The formula is designed to include the mechanical and electrical wear effects and is reported here:

$$NWR = k_1\left(\frac{1}{2}\cdot\left(1+\frac{I_c}{I_0}\right)\right)^{-\alpha}\cdot\left(\frac{F_m}{F_0}\right)^{\beta}\cdot\frac{F_m}{H}+k_2\frac{R_c(F_m)\cdot I_c^2}{H\cdot V_0}(1-u)+k_3 u\frac{V_a I_c}{V_0 H_m \rho} \quad (1)$$

The normal wear rate (NWR) is the area of removed material per kilometre run for the contact strip or the volume of removed material per million contact strip passages for the contact wire.

Table 1 explains all the parameters and the variables included in Eq. (1). Tables 2 and 3 in the appendix give a summary of the parameter values chosen for the two models.

This formula was developed mainly from experience gained with the study of contact wire wear in DC. This allows an easier application for the contact wire, even if some adjustments are needed to adapt it to the AC case. For the contact strip, some changes are needed, mainly because of the so-called current lubrication effect. This effect is accounted for in the mechanical term by the variable α, and it is known to be beneficial for the contact wire. However, this is not the case for the contact strip. Thus, it is natural to split the analysis of the two components to consider the different materials. The split provides two separate models representing the contact wire and the contact strip wear. Therefore, in the following, the behaviour of the contact wire and the contact strip is explored separately. However, before examining the model itself, some considerations about the electric resistance behaviour at the contact point need be made.

The second term of Eq. (1) contains the effects of electrical resistance at the point where the carbon strip and the copper wire are in contact. This term of contact resistance is evaluated as the ratio between the instantaneous voltage drop (v_t) and the electrical current flow (i_t), according to the relation $R_c = v_t/i_t$ [24]. Previous studies [23] have shown how the electric resistance at the contact point is influenced by the value of the force exchanged between the pantograph and the contact wire. To fit the model to the selected conditions, it was chosen to investigate this relation with the data recorded during the tests. Note, however, that the electrical effect on the wear is shared between the time instants where the collector's strip is in contact with the wire and the ones where it is not. Only the data recorded during the contact are used for evaluation in accordance with the formula in Eq. (1). To ensure that the data refer to the time instant where there is no contact loss, a threshold on the voltage signal is set, meaning that, whenever the voltage drop exceeds this limit, an arc is generated, and the corresponding points are discarded.

The data needed for this step are the voltage, current intensity and vertical contact force. The recorded value for the vertical force is the sum of the data coming from two vertical load cells mounted at the collector supports. When using data from load cells in such positions, it is essential to consider the inertia correction. This is needed because the recorded force is the sum of the contact force and the inertia given by the vertical motion of the contact strip. To correct the force signal, only the frequencies associated with the rigid body motion in the vertical plane are considered. For this reason, a low-pass filtering operation is applied to both the force and the acceleration signals. Once the values of the contact resistance and contact force are assessed, it is possible to find the relation between them.

Fig. 2 shows the distribution of the data points corresponding to the contact resistance vs the contact force value pairs. The 3D histogram highlights the proximity of most of the points around low contact resistance values. Various attempts to fit the data points with an exponential function have been made without encouraging results. Regardless of the type of chosen exponential function, within the area of interest, the behaviour was constant. Thus, a linear function of the type $y = a - bx$ was chosen to fit the contact resistance vs contact force curve.

The reason for considering an inverse relationship between contact resistance and force is found in the contact resistance value distribution for different contact force values. Fig. 3 shows how the peak of the contact resistance distribution shifts towards lower values with increasing force.

The resulting function, used both in the model for the contact wire and for the contact strip wear, is as follows:

Table 1
List of the variables and the parameters used in Eq. (1).

Symbol	Description
k_1	Weight of the mechanical wear contribution
α	Coefficient for the dependency of the mechanical wear on the current intensity
β	Coefficient for the dependency of the mechanical wear on the force value
k_2	Weight of the electrical wear contribution
k_3	Weight of the arc wear contribution
F_m	Contact force mean value
F_0	Contact force reference value
I_c	Current intensity nominal value
I_0	Current intensity reference value
V_0	Sliding speed reference value
R_c	Electrical contact resistance between the contact strip and the contact wire
u	Percentage of the contact loss
H	Material hardness
H_m	Material latent heat of fusion
ρ	Material density
V_a	Electrical arc voltage

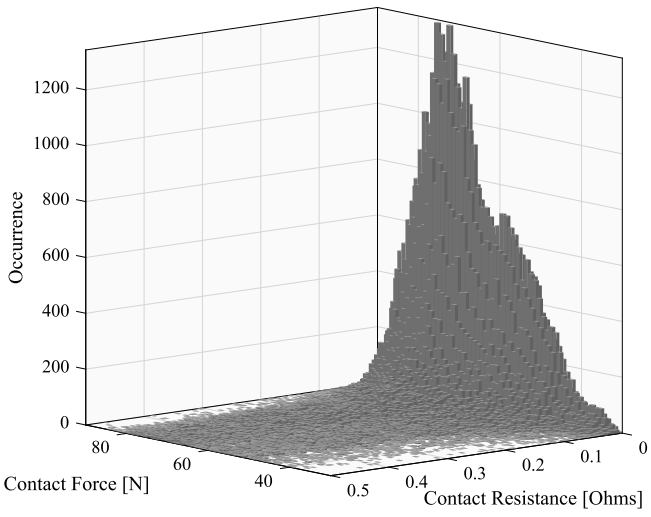

Fig. 2. Contact Resistance vs Contact Force histogram, showing the distribution of the values for this relation.

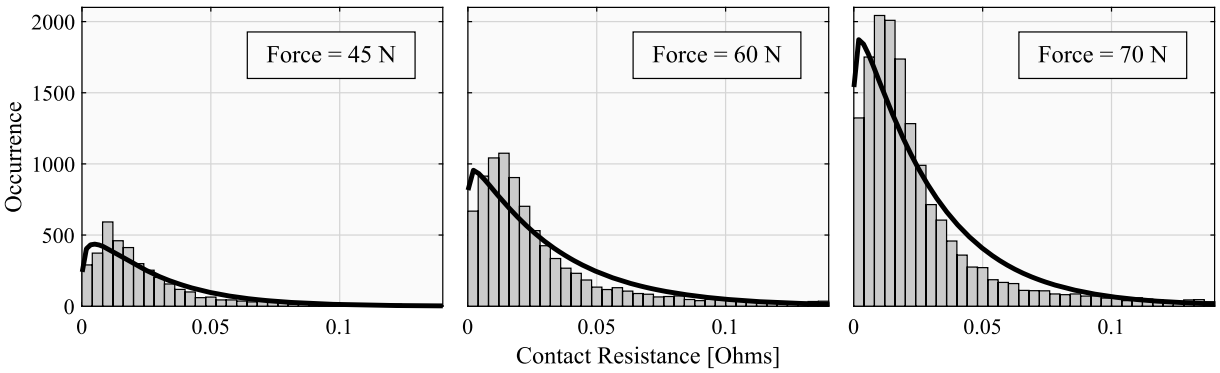

Fig. 3. Contact resistance distribution over three different contact force values. The peaks for the gamma distribution (best fit to the available data) fitted in all three cases are located at the following values of contact resistance: 4.9e-3 for F = 45 N, 2.1e-3 for F = 60 N, 1.9e-3 for F = 70 N.

$$R_c = 0.3276 - 3.47 \cdot 10^{-3} \cdot F \quad (2)$$

4. Contact wire wear model

The first model was built on the wear data associated with the contact wire. The existing literature [19] showed a possible behaviour for a similar type of contact wire, but in that case, the test was performed under DC feeding. The need for a model specifically for AC feeding is clear when looking at the order of magnitude of the wear under the same conditions of current intensity, force and speed. For the AC case, the wear is at least one order of magnitude lower.

The modelling procedure is based on the least square method applied between the measured wear and Eq. (1) evaluated for the same combination of force and current. A sensitivity analysis for each of the parameters was performed to find the underlying structure of the function minimum search instead of letting the algorithm find all five parameters at once. It was found that the sensitivity analysis was beneficial since it allowed to avoid choosing a set of initial conditions for the optimization problem. The function itself has a high degree of nonlinearity and possibly has multiple local minima. Therefore, the choice of random initial conditions might lead to one of the local minima, preventing the algorithm from finding the best achievable result. The method used for the sensitivity analysis consisted of assigning a value to one of the parameters and letting the algorithm find the values for the other four to reach a minimum. At every iteration, the fixed parameter had its value stepwise increased, and the procedure was repeated up to a value far beyond the physics of the problem.

The result of this analysis was satisfying since regardless of which parameter was assigned, the final set of five parameters giving the function minimum was always the same. Furthermore, the minimization function value was the same for all cases. As a result, the set of five values common to all analyses was chosen as the set of values to be used in the surface equation. Further analysis of all the values shows how this is effectively a minimum point.

Once all the parameters are decided, the wear surface representing the dependency on contact force and current intensity is determined, as shown in Fig. 4. The final set of parameters is as follows:

- $k_1 = 0.4921$
- $\alpha = 17.1235$
- $\beta = 0.2119$
- $k_2 = 0.4626$
- $k_3 = 29.6836$

It is important to note that despite the high value assigned to the k_3 coefficient, the arc component still plays a minor role in the overall contribution. The low contribution of the arc component is due to the typical values of percentage of contact loss u. Concerning the mechanical contribution, it is predominant in the area of a high contact force and low electrical current, while for the electrical term, it is exactly the opposite, with the main contribution given in the corner corresponding to a high current and low contact force.

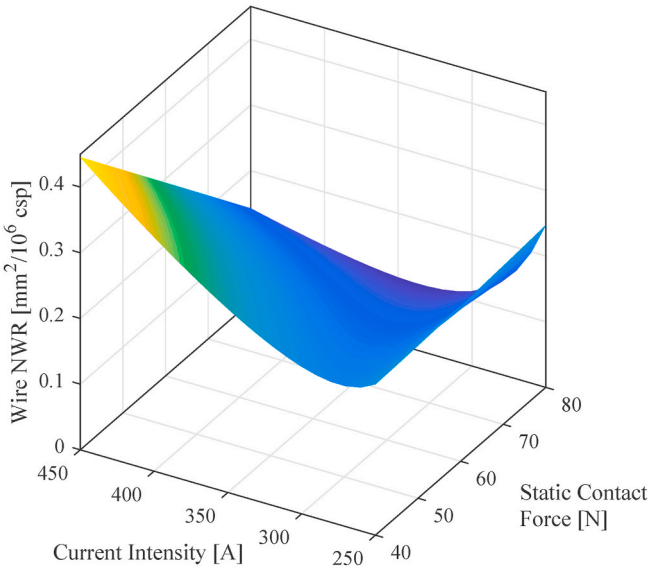

Fig. 4. Net wear rate surface for the CuAg contact wire.

Fig. 5 shows the NWR trends for three different values of contact force, chosen among the values representing the tests to compare the built model with the results from the laboratory. Here, it is also possible to observe the contribution from each component in Eq. (1) to the overall result. The diagrams underline the different areas where mechanical and electrical wear are predominant for high forces and low current and for low forces and high currents.

Fig. 6 shows photographs of the wire surface in two different sections after a series of tests. Fig. 6(a) represents a portion of the wire where mechanical wear is predominant. The lines due to the abrasive action of the contact strip are visible on the surface. Fig. 6(b) shows a wire section where electrical wear and arcs are predominant. The surface colour and the presence of pitting suggest the presence of a significant number of arcs during the test run. The difference in the wear type depending on the wire section is due to the different stiffness values along the test rig wire corresponding to the presence or absence of the wire supports. These variations in stiffness are related to the variations of contact force, which translates ultimately in variations of the contribution given by each component to the wear.

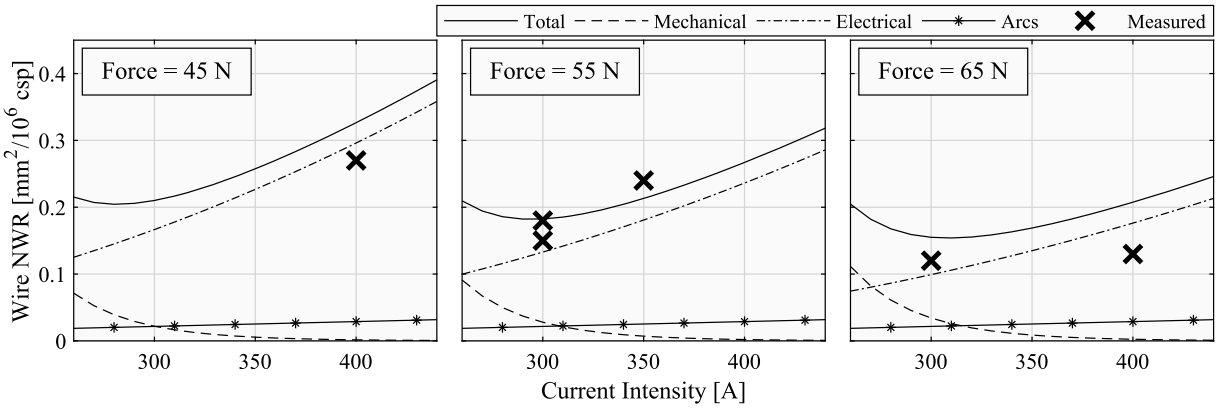

Fig. 5. NWR of the contact wire for three values of contact force; each plot shows the total wear, the components and the measured data. Measured data for the contact wire have an accuracy of 10%.

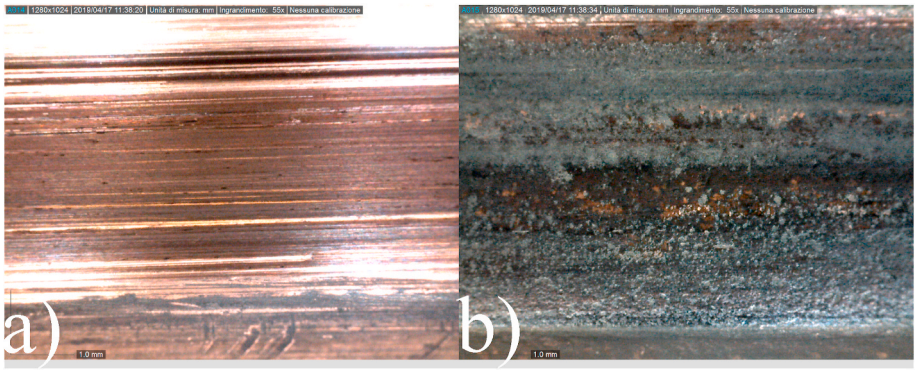

Fig. 6. Copper-silver contact wire after wear test: (a) section where mechanical wear is predominant and (b) section where electrical and arc wear is predominant.

5. Contact strip wear model

The same fitting procedure via Eq. (1) around the measured points was performed on the results from the contact strip wear analysis. The same sensitivity analysis used for the wire was also applied here. However, for the contact strip case, the train speed proved to have a more significant influence on the wear values than for the contact wire case. The NWR values for the tests performed at 210 km/h were of an order of magnitude higher than the corresponding tests performed at either 130 km/h or 160 km/h. For this reason, only tests at higher speeds were considered for the surface fitting.

The properties of the Cu-impregnated carbon strip were chosen based on an X-ray diffraction analysis carried out on one of the contact strips used for the test.

The procedure to analyse the effect of each of the parameters on the overall minimization of the contact strip wear gave results that need to be studied more thoroughly than the contact wire case. The effects of model parameters on the two sides of the contact are in fact different due to the diverse nature of the materials involved. An example of this asymmetry in the behaviour is the current lubrication effect, represented by the coefficient α. An increase in current increases the lubrication, hence decreasing the mechanical wear. However, this effect is beneficial mainly for the copper wire. A new sensitivity analysis was performed to better understand which components have the most influence on the overall minimization. This time, every component of the surface equation was tested, first alone and then in a few configurations with the others. The criterion to assess the fitting quality remained the minimization function value.

After assessing each component individually, the resulting outcome indicated that the best model was the one where arcs were predominant. The same outcome also indicated that the mechanical component was the least meaningful. This result was not in line with existing knowledge of the phenomenon. Thus, the mechanical component was investigated deeper considering the possibility of a different behaviour than the wire case. Two separate sensitivity analyses were conducted with the effects of the force and current lubrication removed. The final results show that the analysis that excludes the current lubrication effect from the formula has the best fit. This finding has a very clear physical meaning since only the wire can benefit from the lubrication occurring in the presence of electric current. This is because the lubricant is carbon from the contact strip, which implies more severe wear for the carbon strip than for the copper wire. The final surface for the carbon strip does not show the same clear distinction among the different operating conditions as for the wire. This is a consequence of excluding the exponential term in the mechanical component of Eq. (1). Fig. 7 shows the model, obtained with the following set of coefficients:

- $k_1 = 6.650$
- $\alpha = 0$
- $\beta = -0.450$
- $k_2 = 4.995$
- $k_3 = 3230$

To better understand the effects of single components on the overall result for the contact strip (as was done for the contact wire), the trend for each of them is shown in Fig. 8. In addition, the measured values for the wear obtained in the 210 km/h tests are shown as crosses overlapping with the model.

The electrical component is found to play a major role, even though the corresponding coefficient k_2 has a lower value than the other two components. The constant behaviour of the mechanical component along the current intensity axis is justified by the removal of the

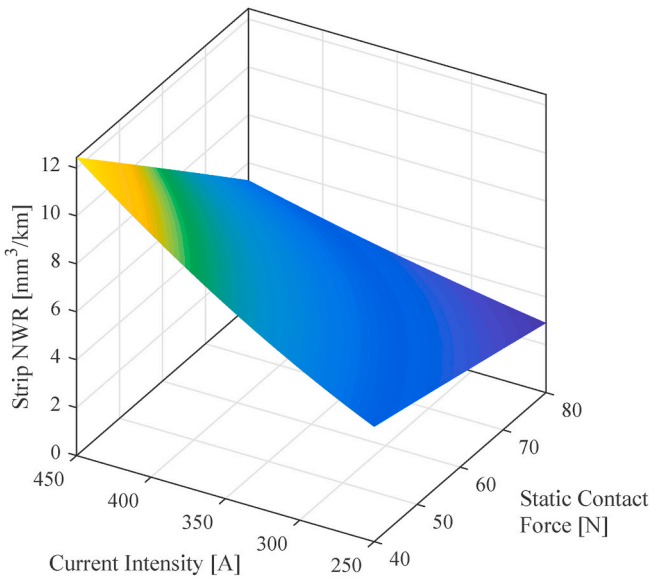

Fig. 7. Net wear rate surface for the Cu-impregnated carbon contact strip.

coefficient α. The behaviour along the force axis shows a slight positive trend for increasing values of force.

Fig. 9 shows photographs of the contact strip after a test. Fig. 9(a) shows the top surface where longitudinal marks due to mechanical wear are visible, together with pits associated with the presence of arcs. Fig. 9 (b) shows the trailing side of the contact strip exhibiting wear due to the electrical effects. Arcs can strike both on the top surface and on the trailing side due to the air generated by the train speed and reproduced during the tests.

6. Model comparison

The method used for this work was refined during the execution of the test campaign. This refinement was enabled by the analysis of the results, which gave new information about the specific setup at the end of each test. The main consequence was to introduce a clear distinction between the contact strip and the contact wire behaviour, which led to the separate analysis of the two components and, hence, the generation of two different models. This result was due to the initial unsatisfactory fitting procedure when using the same equation for both components, despite a general trend that looked very similar for some operating conditions.

Regarding the contact wire, the presence of previous successful results in the literature made it possible to use the model as is. For the contact strip, on the other hand, the wear formula was tuned specifically for this case. The most suitable option was a model where the current lubrication effect was disregarded. This model was identified after a more detailed analysis was conducted regarding the influence of each term of the equation on the outcome of the fitting procedure.

Since both components have to work under the same operating conditions, it is important to understand what combination of current and force values provides the best results. Wear cannot be avoided, but it can be controlled in a way that potentially satisfies both the infrastructure owner and the train operators.

The model for the contact wire leads to a straightforward conclusion with respect to the operating conditions. Mechanical and electrical wear are in fact predominant in two distinct areas of the current intensity/

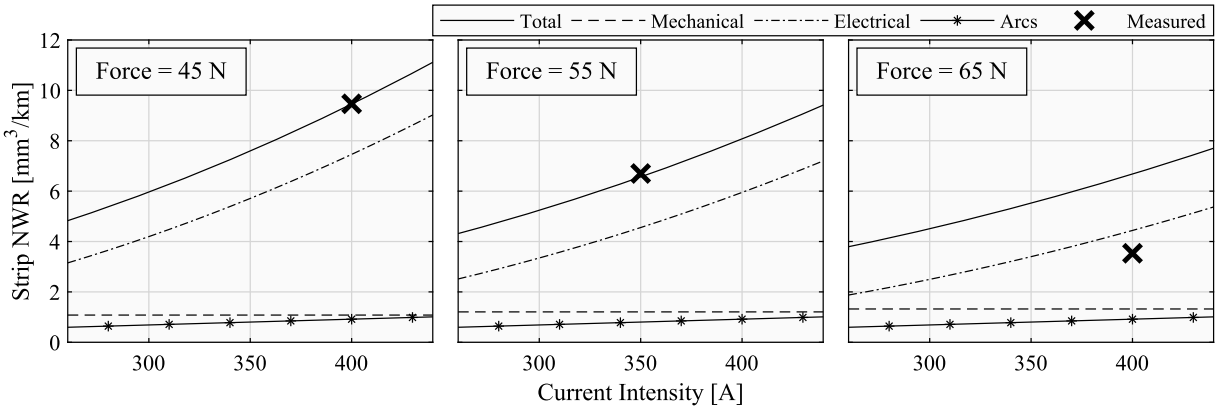

Fig. 8. NWR of the contact strip for three values of contact force; each plot shows the total wear, components and measured data. Measured data for the contact strip have an accuracy of 1%.

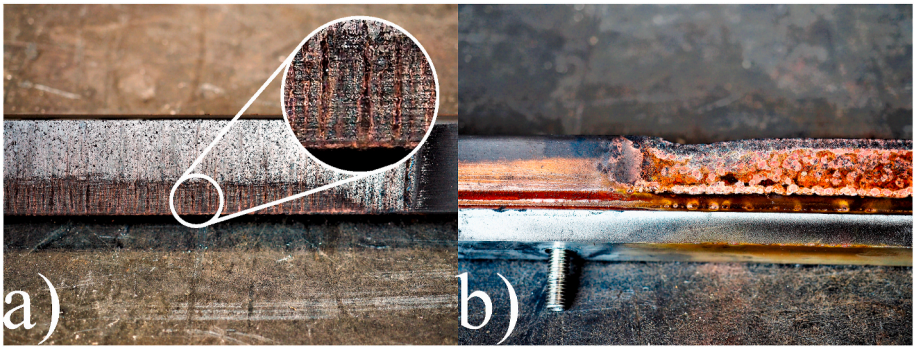

Fig. 9. Cu-impregnated carbon contact strip after wear test: a) top surface with both the effects of mechanical abrasion (highlighted in the white circle) and arcs and b) trailing side with mainly the effects of the arcs.

contact force domain. The wear for low-force and high-current operating conditions is dominated by the electrical component, while for high-force and low-current operating conditions, the wear is mainly mechanical. Between these two areas, a minimum point is found where the wear is low.

The same conclusion cannot be made for the contact strip. In this case, the general trend is one of low wear for low-current operating conditions, mainly because of the avoidance of carbon melting when the Joule effect is moderate. The dependency on the contact force is less explicit than for the contact wire but shows a decrease in wear with increasing force due to the lower influence of arcs on the wear.

7. Conclusions

This paper shows a procedure to obtain a model for the wear in pantograph-catenary contact interaction. The main goal is to provide a heuristic model for the wear of both the contact wire and the contact strip. The working conditions for the models are a 15 kV 16.67 Hz AC catenary system and a Cu-impregnated contact strip. Notably, the wear is highly dependent on such operating conditions and on the material chosen for the contact wire and contact strip. Thus, a model tuned on a specific couple of contact wire and contact strip further increases the understanding of the wear phenomenon on the two components.

The described procedure led to two different models, one for the copper-silver 100 mm^2 contact wire and one for the copper-impregnated carbon contact strip. Both models are based on tuning the same formula as presented in Eq. (1) to the measured results for each case. These models are useful for multiple purposes:

- Wear models can be used together with a pantograph-catenary interaction numerical model to predict the wear of both components in the case of long-duration simulations. It is important to take the proper wear into account since changes in the geometry and mass change the dynamic behaviour of the system. This type of simulation can be of particular interest for newly designed lines to tune the parameters to match a wear level that guarantees the required reliability;
- For existing lines, the wear model can be used together with statistical data of the current, contact force and line speed retrieved from field measurements to predict the wear when operations are carried on along a railway line;
- Another use for the existing lines can be in the case of choosing operating conditions. The wear model makes it possible to decide under which level of wear each component operates, thus providing acceptable values for both the infrastructure and the railway vehicle.

Declaration of competing interest

The authors declare that they have no known competing financial interests or personal relationships that could have appeared to influence the work reported in this paper.

CRediT authorship contribution statement

Stefano Derosa: Conceptualization, Methodology, Software, Validation, Formal analysis, Investigation, Data curation, Writing - original draft, Visualization. **Petter Nåvik:** Conceptualization, Methodology, Resources, Writing - review & editing. **Andrea Collina:** Methodology, Resources, Writing - review & editing. **Giuseppe Bucca:** Conceptualization, Methodology, Software, Validation, Investigation, Data curation, Writing - review & editing, Visualization. **Anders Rønnquist:** Methodology, Validation, Resources, Writing - review & editing, Supervision, Project administration, Funding acquisition.

Acknowledgments

The authors are grateful to the Norwegian Railway Directorate for the funding of this research.

Appendix

Table 2
List of the parameters used in Eq. (1) for the contact wire model

Symbol	Description	Value
k_1	Weight of the mechanical wear contribution	0.4921
α	Coefficient for the dependency of the mechanical wear on the current intensity	17.1235
β	Coefficient for the dependency of the mechanical wear on the force value	0.2119
k_2	Weight of the electrical wear contribution	0.4626
k_3	Weight of the arc wear contribution	29.6836
F_0 [N]	Contact force reference value	60
I_0 [A]	Current intensity reference value	300
V_0 [m/s]	Sliding speed reference value	44.44
H [N/m^2]	Material hardness	952
H_m [J/kg]	Material latent heat of fusion	205×10^3
ρ [kg/m^3]	Material density	8940
V_a [V]	Electrical arc voltage (from Ref. [23])	15

Table 3
List of the parameters used in Eq. (1) for the contact strip model

Symbol	Description	Value
k_1	Weight of the mechanical wear contribution	6.65
α	Coefficient for the dependency of the mechanical wear on the current intensity	0
β	Coefficient for the dependency of the mechanical wear on the force value	−0.45
k_2	Weight of the electrical wear contribution	4.995
k_3	Weight of the arc wear contribution	3230
F_0 [N]	Contact force reference value	58
I_0 [A]	Current intensity reference value	350

(*continued on next page*)

Table 3 (*continued*)

Symbol	Description	Value
V_0 [m/s]	Sliding speed reference value	58.33
H [N/m^2]	Material hardness	311
H_m [J/kg]	Material latent heat of fusion	1700×10^3
ρ [kg/m^3]	Material density	3000
V_a [V]	Electrical arc voltage (from Ref. [23])	15

References

[1] S. Bruni, G. Bucca, M. Carnevale, A. Collina, A. Facchinetti, Pantograph–catenary interaction: recent achievements and future research challenges, Int. J. Rail Transport. (2017) 1–26, https://doi.org/10.1080/23248378.2017.1400156, 00.

[2] H. Borgwardt, Verschleiß Verhalten des Fahrdraht der Oberleitung, Elektr. Bahnen 87 (1989) 287–295.

[3] P. Nåvik, A. Rønnquist, S. Stichel, The use of dynamic response to evaluate and improve the optimization of existing soft railway catenary systems for higher speeds, Proc. Inst. Mech. Eng. - Part F J. Rail Rapid Transit 230 (2015) 1388–1396, https://doi.org/10.1177/0954409715605140.

[4] M. Bocciolone, A. Collina, G. Bucca, F. Mapelli, A Test Rig for the Comparative Evaluation of the Performance of Collector Strips, 2004.

[5] S. Bruni, G. Bucca, A. Collina, A. Facchinetti, S. Melzi, Pantograph-catenary dynamic interaction in the medium-high frequency range, Veh. Syst. Dyn. 41 (2004) 697–706.

[6] K. Becker, A. Rukwied, W. Zweig, U. Resch, Simulation of the wear behaviour of high-speed over-head current collection systems, Trans. Built Environ. 17 (1996) 281–290.

[7] D. Klapas, F.A. Benson, R. Hackam, Simulation of wear in overhead current collection systems, Rev. Sci. Instrum. 56 (1985) 1820–1828, https://doi.org/10.1063/1.1138101.

[8] D. Klapas, F.A. Benson, R. Hackam, P.R. Evison, Wear in simulated railway overhead current collection systems, Wear 126 (1988) 167–190, https://doi.org/10.1016/0043-1648(88)90136-6.

[9] A. Senouci, J. Frene, H. Zaidi, Wear mechanism in graphite-copper electrical sliding contact, Wear 225–229 (1999) 949–953, https://doi.org/10.1016/S0043-1648(98)00412-8.

[10] G. Bucca, A. Collina, E. Tanzi, Experimental analysis of the influence of the electrical arc on the wear rate of contact strip and contact wire in a.c. System, Int. J. Mech. Control 18 (2017) 449–456, https://doi.org/10.1007/978-3-319-48375-7_48.

[11] S. Kubo, K. Kato, Effect of arc discharge on wear rate of Cu-impregnated carbon strip in unlubricated sliding against Cu trolley under electric current, Wear 216 (1998) 172–178, https://doi.org/10.1016/S0043-1648(97)00184-1.

[12] T. Ding, G.X. Chen, X. Wang, M.H. Zhu, W.H. Zhang, W.X. Zhou, Friction and wear behavior of pure carbon strip sliding against copper contact wire under AC passage at high speeds, Tribol. Int. 44 (2011) 437–444, https://doi.org/10.1016/j.triboint.2010.11.022.

[13] S. Kubo, K. Kato, Effect of arc discharge on the wear rate and wear mode transition of a copper-impregnated metallized carbon contact strip sliding against a copper disk, Tribol. Int. 32 (1999) 367–378, https://doi.org/10.1016/S0301-679X(99)00062-6.

[14] H. Nagasawa, K. Kato, Wear mechanism of copper alloy wire sliding against iron-base strip under electric current, Wear 216 (1998) 179–183, https://doi.org/10.1016/S0043-1648(97)00162-2.

[15] Y. Kubota, S. Nagasaka, T. Miyauchi, C. Yamashita, H. Kakishima, Sliding wear behavior of copper alloy impregnated C/C composites under an electrical current, Wear 302 (2013) 1492–1498, https://doi.org/10.1016/j.wear.2012.11.029.

[16] D.H. He, R.R. Manory, N. Grady, Wear of railway contact wires against current collector materials, Wear 215 (1998) 146–155, https://doi.org/10.1016/s0043-1648(97)00262-7.

[17] S.C. Lim, M.F. Ashby, Wear-Mechanism maps, Acta Metall. 35 (1987) 1–24, https://doi.org/10.1016/0001-6160(87)90209-4.

[18] G. Bucca, A. Collina, A procedure for the wear prediction of collector strip and contact wire in pantograph-catenary system, Wear 266 (2009) 46–59, https://doi.org/10.1016/j.wear.2008.05.006.

[19] G. Bucca, A. Collina, Electromechanical interaction between carbon-based pantograph strip and copper contact wire: a heuristic wear model, Tribol. Int. 92 (2015) 47–56, https://doi.org/10.1016/j.triboint.2015.05.019.

[20] A. Collina, S. Melzi, A. Facchinetti, On the prediction of wear of contact wire in OHE lines: a proposed model, Veh. Syst. Dyn. 37 (2002) 579–592, https://doi.org/10.1080/00423114.2002.11666264.

[21] G.X. Chen, H.J. Yang, W.H. Zhang, X. Wang, S.D. Zhang, Z.R. Zhou, Experimental study on arc ablation occurring in a contact strip rubbing against a contact wire with electrical current, Tribol. Int. 61 (2013) 88–94, https://doi.org/10.1016/j.triboint.2012.11.020.

[22] A. Rønnquist, P. Nåvik, Dynamic assessment of existing soft catenary systems using modal analysis to explore higher train velocities: a case study of a Norwegian contact line system, Veh. Syst. Dyn. 53 (2015) 756–774, https://doi.org/10.1080/00423114.2015.1013040.

[23] G. Bucca, A. Collina, R. Manigrasso, F. Mapelli, D. Tarsitano, Analysis of electrical interferences related to the current collection quality in pantograph-catenary interaction, Proc. Inst. Mech. Eng. - Part F J. Rail Rapid Transit 225 (2011) 483–499, https://doi.org/10.1177/0954409710396786.

[24] J.A. Bares, N. Argibay, P.L. Dickrell, G.R. Bourne, D.L. Burris, J.C. Ziegert, et al., In situ graphite lubrication of metallic sliding electrical contacts, Wear 267 (2009) 1462–1469, https://doi.org/10.1016/j.wear.2009.03.024.